Supporting information

Shell-Binary Nanoparticle Materials with Variable Electrical and Electro-mechanical Properties

*Pengcheng Zhang, Herbert Bousack, Yang Dai, Andreas Offenhäusser, Dirk Mayer**

Institute of Complex Systems, Bioelectronics (ICS-8) and JARA – Fundamentals of Future Information Technology, Forschungszentrum Jülich, 52425 Jülich, Germany

*Corresponding Author: Email: dirk.mayer@fz-juelich.de

Table of Contents

1. Materials

11-mercaptoundecanoic acid (MUA), bis (p-sulfonatophenyl) phenylphosphine dihydrate dipotassium salt (BSPP), sodium tris-citrate ($Na_3C_4H_5O_7$), sodium hydroxide (NaOH), gold (III) chloride hydrate($HAuClO_4$) were purchased from Sigma-Aldrich and were used as received.

2. STEM images of CIT-AuNPs, BSPP-AuNPs and MUA-AuNPs

Particle sizes were characterized by scanning transmission electron microscopy (STEM) and a particle diameter of 17.5±1.9 nm was obtained for CIT-AuNPs sample.

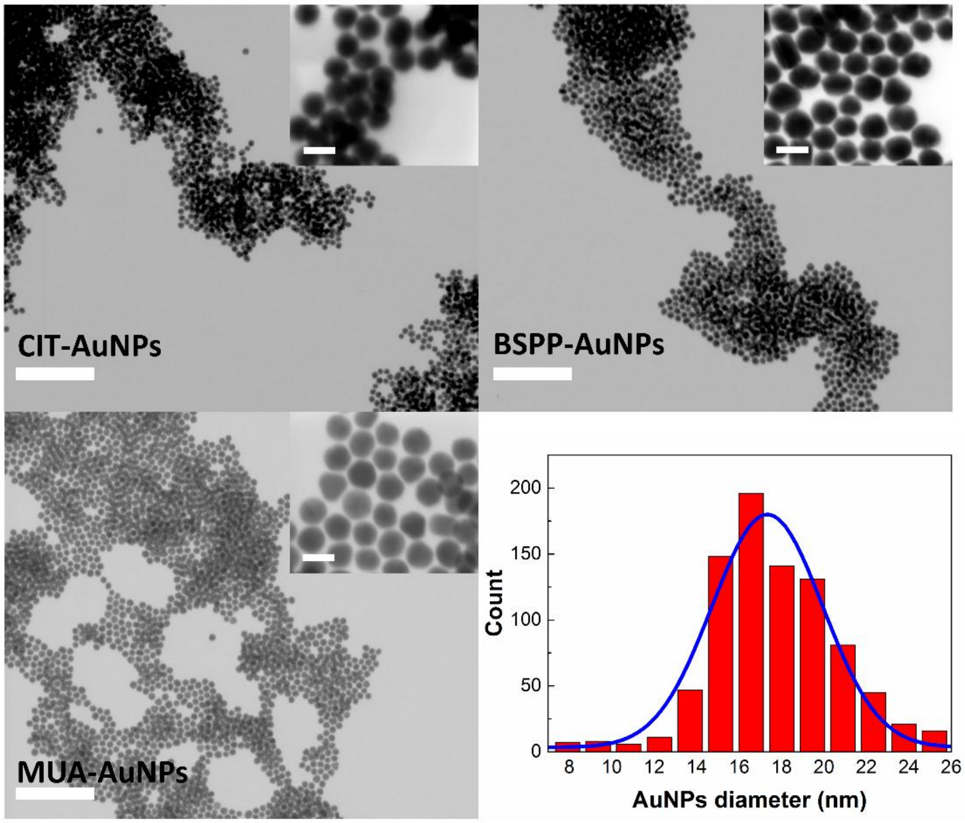

Figure S1. STEM images of the CIT-AuNPs, BSPP-AuNPs, MUA-AuNPs and the size distribution of the CIT-AuNPs. Scale bar: 200nm and 20nm (insert).

3. **UV-Vis spectroscopy of the CIT-AuNPs, BSPP-AuNPs and MUA-AuNPs solution after concentration process**

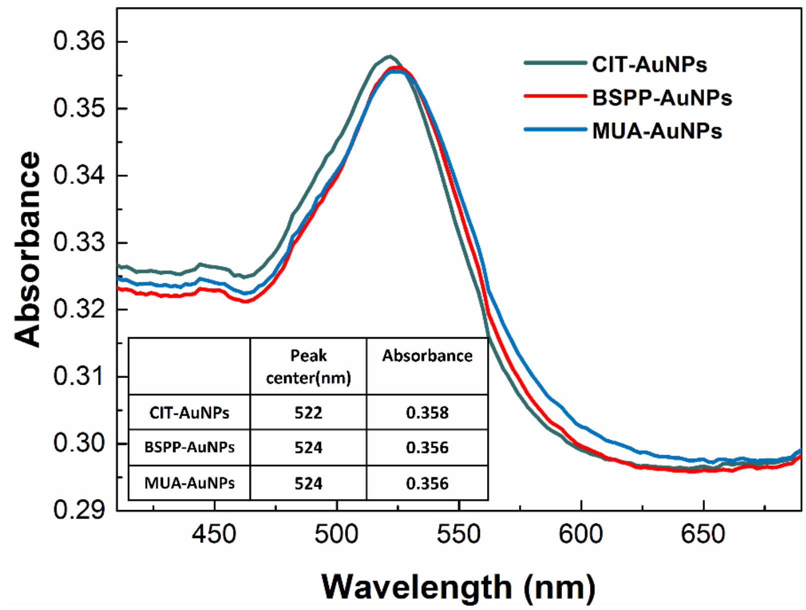

Figure S2. UV-Vis spectroscopy of the CIT-AuNPs, BSPP-AuNPs and MUA-AuNPs solution after concentration process.

4. **CSA process and SBNMs stripes fabrication**

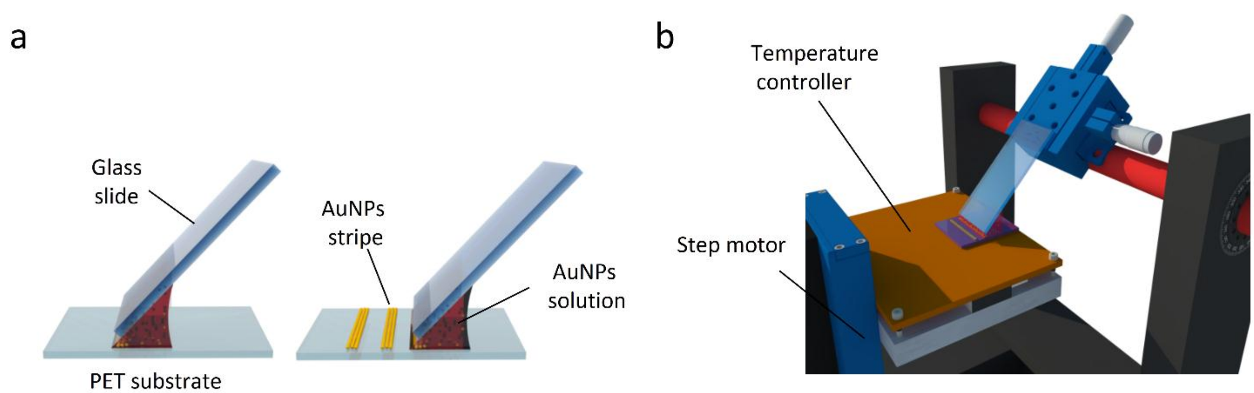

Figure S3. a: schematic of CSA process. b: homemade CSA setup.

The convective self-assembly (CSA) process and setup is shown in Figure S3. Si/SiO_2 substrate and PET films with 125μm in thickness (Pütz GmbH) were used for depositing the SBNMs stripes. All the substrates were cleaned twice with ethanol and 2-proponal, rinsed with ultra-high-purity water, and dried in a stream of nitrogen. The homemade CSA setup consists of a rectangular glass slide inclined at an angle of 45° over the horizontal substrate fixed to a temperature-regulated copper plate. The copper plate was controlled at 35°C during the CSA process. The CSA process was carried out in an ambient environment with a surrounding temperature of 22 °C and a humidity of ~45%RH. Before CSA, the substrates and glass slides were treated by O_2 plasma (80W, 0.8mbar) for 3min. 30μl of AuNPs mixture solution was injected into wedge formed between the glass slide and the substrate. The meniscus formed by the AuNPs mixture solution with the substrate was translated across the substrate at a speed v = 100 $\mu m \cdot s^{-1}$ by a computer controlled step motor. The stop time is 20s for each AuNPs stripe. The distance between each stripe is 50μm.

5. **Optical microscopy, AFM and laser microscopic characterizations of the SBNMs stripes**

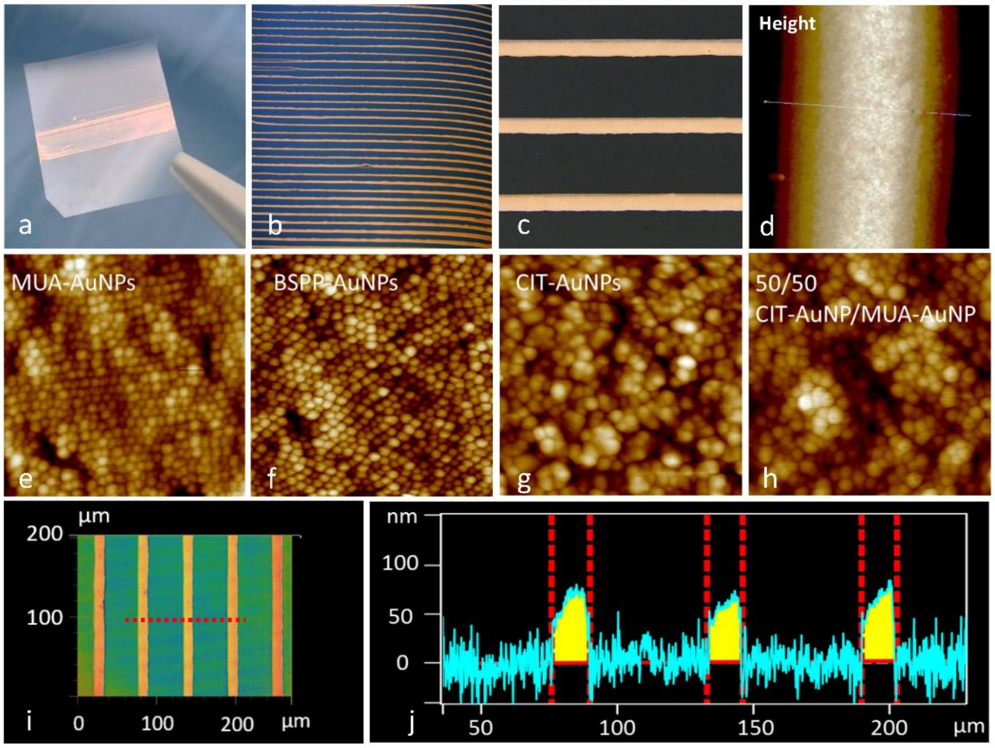

Figure S4. a-c: optical microscopy images of stripes on PET substrate. d: AFM amplitude image of a single stripe. e-g: AFM images of stripes consisting of different AuNPs or binary AuNPs on PET substrate. The AFM images show areas of (500×500) nm^2. i, j: laser microscope images of AuNPs stripes on PET substrate. The yellow areas in image j show the cross-section areas of individual stripe.

The morphologies and dimensions of the AuNPs stripes were investigated by optical microscopy (Zeiss), tapping mode atomic force microscopy (AFM) (Nanoscope), and laser microscopy (Keyence). AFM images show the AuNPs stripes composed of single component AuNPs materials (MUA-AuNPs, BSPP-AuNPs or CIT-AuNPs) and the binary AuNPs materials (CIT-AuNP/MUA-AuNP$_{50/50}$). The stripes composed of MUA-AuNPs (Figure S4e) and BSPP-

AuNPs (Figure S4-f) show an ordered pattern. However the stripes of CIT- containing AuNPs (Figure S4-g, h) possess aggregations. This indicates that the citrate protecting layer cannot completely suppress aggregation during the assembly process. For calculating the conductivity of the AuNPs stripes, dimensions of the stripes were determined by the laser microscopy. Figure S5-j shows the cross section and the area of individual AuNPs stripe.

6. **Monte Carlo simulation on the percolation threshold in SBNMs stripe with different dimensions**

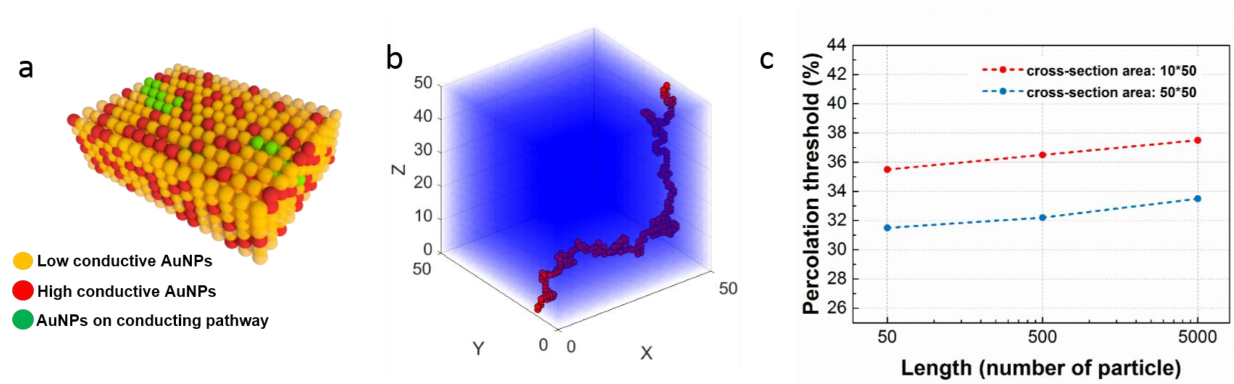

Figure S5. a: schematic of close packed cubic lattice pattern. The different colors of the AuNPs stand for the different AuNPs species as indicated in the images. b: conduction pathway in a 50×50×50 cubic lattice (volume fraction is 50%). The red spheres indicate the particles on the conduction pathway along the +x direction. c: simulated conductive percolation threshold for different strip dimensions. The different slopes of the curve can be ascribed to the different quantities of the spheres in different dimensions. With numbers of the spheres increasing, the slopes of the curve become more close to +∞, at which the value of the abscissa indicates the percolation threshold. d: percolation threshold value in different cross-section area and length, which are extracted from Figure 4(a) in the main article.

A three-dimensional (3D) Monte Carlo algorithm was used to determine the conductive percolation threshold of SBNMs stripes composed of two kinds of spheres (standing for highly conducting and low conducting nanoparticles, Figure S5-a). These spheres are arranged in a closed packed cubic lattice pattern and randomly located on each lattice site. The algorithm based on Depth-First Search (DFS) was used to search the conducting pathways for each mixing ratio. The percolation probability then can be obtained for different times (n=100 in this work) of simulations. As a test, a simple cubic lattice with dimension of 50×50×50 was simulated (Figure S7-a) and the percolation threshold of ~31% was obtained, which is in good agreement with the reference value [1]. As in the experiment, the actual AuNPs stripes fabricated by CSA are slender stripes. To study the dimension dependent percolation threshold, cubic lattices with different cross-section (10×50 and 50×50) and length (50, 500, and 5000) were simulated (Figure S5-c). The results show that the percolation threshold increases as the cross-section of the stripes decreases or the length of the stripes increases, (Figure S5-c). The stripes dimension with cross-section of 10×50 and length of 500 represents a good approximation to the actual stripes used in these experiments. For this example (10×50×5000), a threshold value of ~37% was obtained, which is in good agreement with the experimental value obtained for the BSPP-AuNP/MUA-AuNP ho-SBNMs (~35%). This indicated that the threshold of the SBNMs can be shifted by varying the dimension of the stripes. As the dimension turns into the slender stripe in the experiment, threshold is shifted to a higher value. One should note that different slopes of the curves in different dimensions (Figure 4(a) in the main article) can be related to the different number of spheres for the respective dimensions. [2]

7. Electro-mechanical measurements

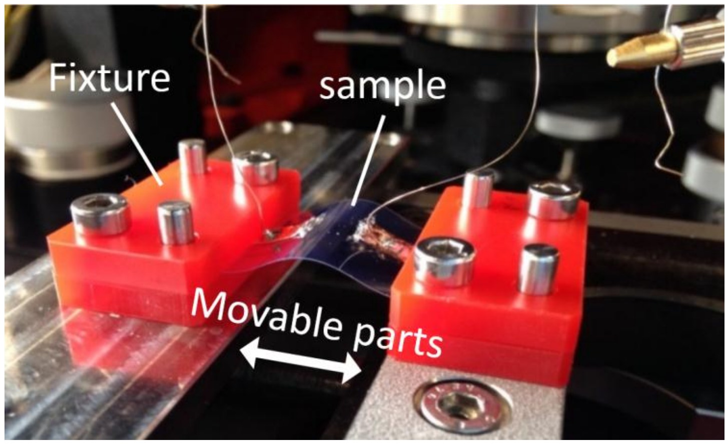

Figure S6. The bending setup.

The bending setup for mechanical measurement is shown in Figure S6. For accuracy, this setup was calibrated by a standard metal foil strain sensor (Hottinger Baldwin Messtechnik GmbH). The sample was fixed on the plastic fixtures and strain ranging from 0% to 0.52% was applied by pushing and bending the strain sensor. The electrical resistance of the sample was measured by a computer-interfaced multichannel meter (Keithley, Model 6200) at a constant voltage of 0.5V, synchronized with the bending of the strain sensor on the setup. Cyclic strain loading and bending tests of the sample were performed in a homemade step motor bending setup at a controlled frequency. All the experiments were performed at room temperature.

8. **Dependence of the GF and conductivity on volume fraction of CIT-AuNPs in CIT-AuNP/MUA-AuNP he-SBNMs.**

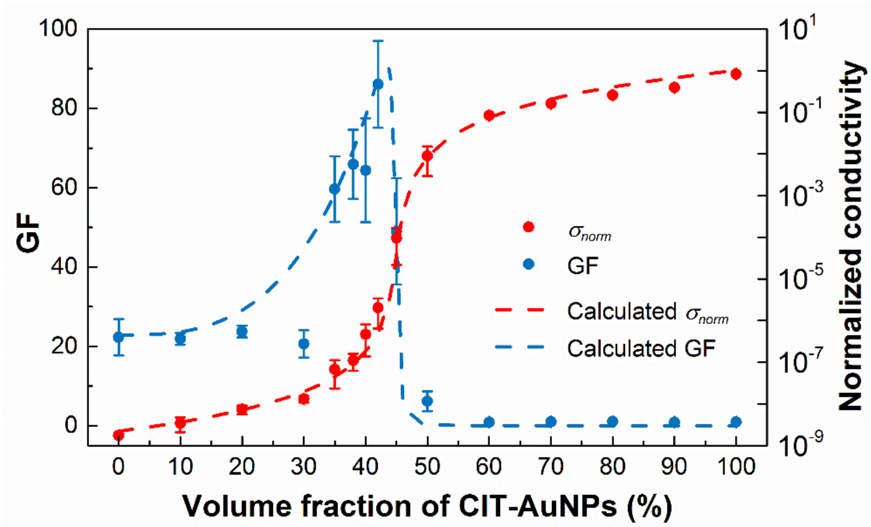

Figure S7. The normalized conductivities σ_{norm} (red dot) and GF value (blue dot) of (a) CIT-AuNP/MUA-AuNP he-SBNMs versus the volume fraction ratio φ. Dash line: calculated conductivities σ_{norm} (red dash line) and GF value (blue dash line) dependence on volume fraction ratio φ. The aggregation coefficient α for fitting of the GF value is 31.2.

9. **The IV measurement and different GF of the SBNMs stripes**

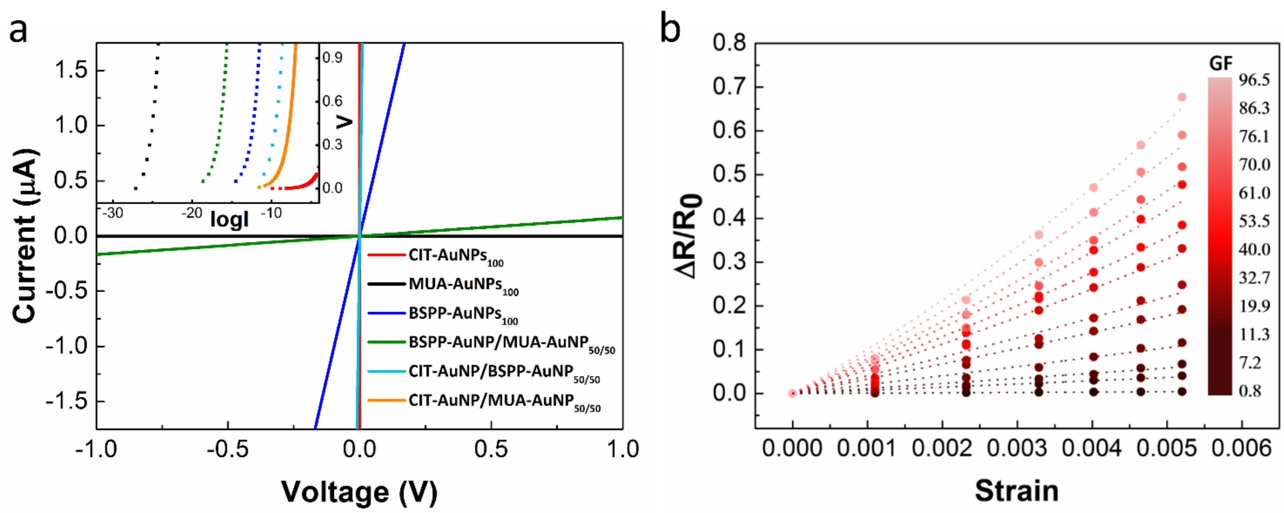

Figure S8. a: IV characteristics for unstrained sample consisting of different single component AuNPs or SBNMs s at 300 K. The inset presents the logI/V curve (tafel plot). b: resistance change versus strain of sample with GF values ranging from 0.8 to 96.5.

The resistances of the unstrained sample based on single component AuNPs (BSPP, MUA or CIT-AuNPs) or SBNMs (CIT-AuNP/BSPP-AuNP, CIT-AuNP/MUA-AuNP or BSPP-AuNP/MUA-AuNP) were measured at room temperature (T=300 K)(Figure S8-a). It is shown that the IV characteristics at room temperature for ±1.0 V sweeps are linear for all samples. SBNMs with fine adjustable GF value can be realized. The resistance changes versus strain of the respective sample are shown in Figure S8-b.

10. Changes of microscopic morphology and 2D auto correlation length ξ caused by variation of particle volume fractions

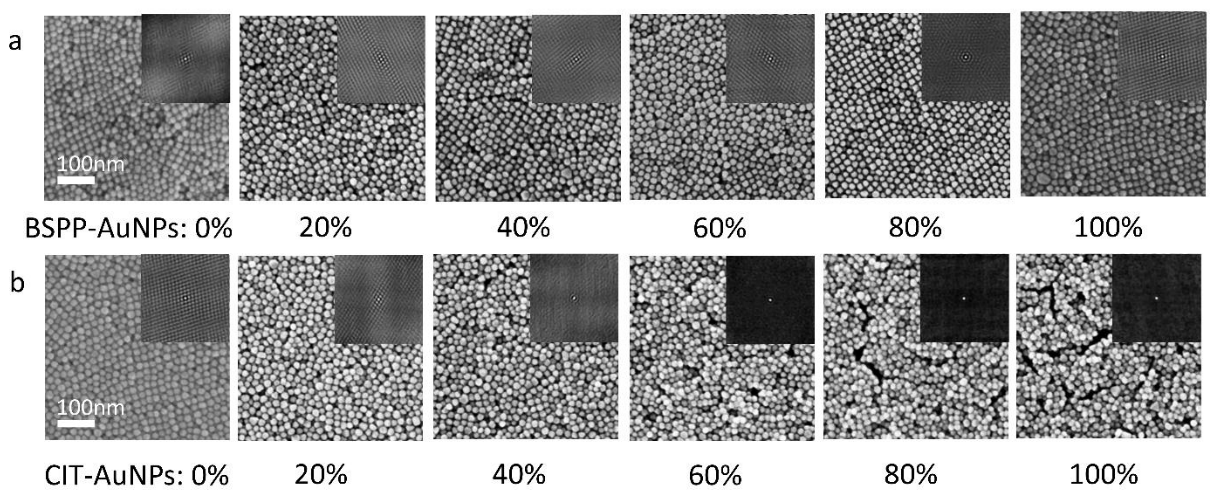

Figure S9. a: SEM images of BSPP-AuNP/MUA-AuNP ho-SBNMs. b: SEM images of CIT-AuNP/BSPP-AuNP he-SBNMs at different volume fraction φ. Inset images show the correspondingly 2D autocorrelation spectrums.

The degree of the AuNPs ordering in the SBNMs were quantitatively described by the correlation length ξ. A detailed description of the determination of ξ from images can be found in references.[3, 4] Briefly, image analysis has been performed on SEM images with an area of (500 × 500) nm^2 (Figure S9). The autocorrelation spectrum of these images was calculated (insets in Figure S9). From the autocorrelation spectra, radial profiles was extracted and equation S(1) was applied to fit the radial profiles.[4] Correlation length ξ then can be deducted from the fitting of the following equation:

$$y = \exp\left(\frac{-x}{\xi}\right)\sin\left(2\pi\frac{x-c}{D}\right) \tag{1}$$

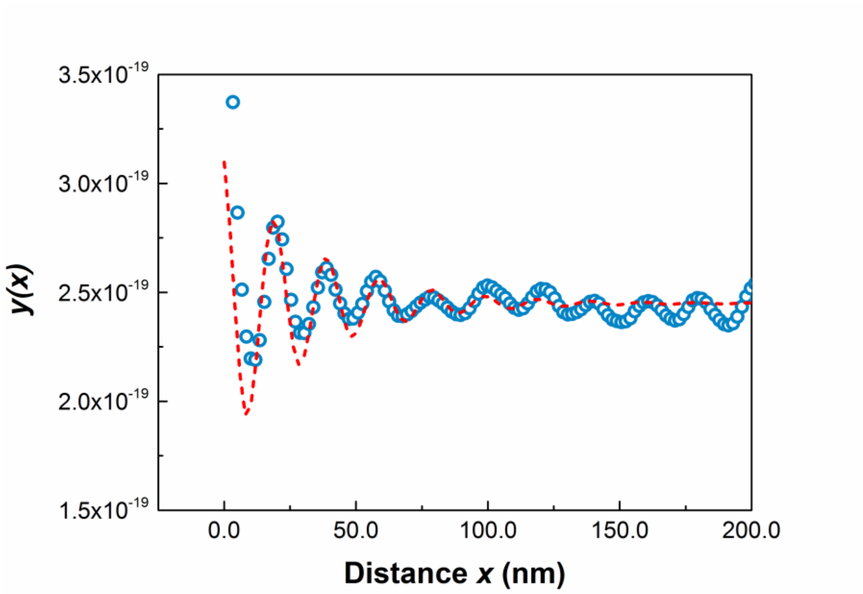

Figure S10. Fitting curve (red dashed line) of radial profile (blue cycles) of BSPP-AuNP/MUA-AuNP$_{80/20}$ ho-SBNMs by equation (1) in supporting information.

11. Effective medium theory, coupling parameter *g* and fitting parameters

The effective medium theory (EMT) was initially developed by Bruggeman to calculate the dielectric constants and polarizabilities of heterogeneous crystalline media.[5] The main approximation is that all the domains of the material are located in an equivalent mean field. Together with other acceptable approximations, EMT provides a model to describe the macroscopic properties of composite materials. Thus, by knowing the properties of the bare components and their relative fractions, the property of the composite material can be derived from calculations. In the SBNMs stripe, the AuNPs represent two kinds of resistors with different tunneling resistances. These resistors are randomly distributed in the stripe. The resulting resistor network can be considered as composite material with two components and thus described by EMT. The overall conductivity of the resistor network can be calculated for different volume fraction ratio of the used AuNPs. As the applied strain changes the tunneling resistances of the resistors, the electro-mechanical properties can be calculated by treating the strain as a perturbation of the overall conductivity.

The tunneling coupling parameter g can be expressed as $g = G/G_0$, where G is the average conductance of the NP junction and G_0 is the quantum conductance $e^2/\hbar$. The value of G can be obtained by using the reciprocal value of the tunneling resistance R_t between the adjacent AuNPs (BSPP junction or MUA junction) or the resistance R_m via direct metallic contact between CIT- AuNPs (CIT junction), as shown in the main article. The threshold values φ_c obtained from the experimental results are 35%, 48% and 45% for BSPP-AuNP/MUA-AuNP, CIT-AuNP/BSPP-AuNP and CIT-AuNP/MUA-AuNP SBNMs stripes, respectively. The parameter t of equation (7) in the main article is 2.5, 1.2 and 2.0 for BSPP-AuNP/MUA-AuNP, CIT-AuNP/BSPP-AuNP and CIT-AuNP/MUA-AuNP SBNMs stripes, respectively. The other fitting parameters are shown in Table S1.

Table S1. Fitting parameters of AuNPs stripes containing different particle ligands (BSPP, MUA and CIT). Conductivity without strain δ (300 K) is obtained from the electrical measurement of the stripes composed of mono phase AuNPs. Molecular length l of the BSPP and MUA are taken from references.[6] Values of A are extracted from equation (4), (5) and (6) in the main article respectively. Values of β are extracted from electro-mechanical measurements based on equation (13).

	δ_{300K} (Scm^{-1})	d (nm)	l (nm)	β (nm^{-1})	g	A (Scm^{-1})		
BSPP-AuNPs	0.22	17.5	0.8	2.1	5.2×10^{-3}	4.0		1.2×10^{-4}
MUA-AuNPs	3.7×10^{-4}	17.5	2	1.1	9.4×10^{-6}	2.0×10^{-5}	2.0×10^{-8}	
CIT-AuNPs	1.3×10^{4}	17.5	-	-	3.0×10^{2}		1.0	1.0

Note that the values of tunneling decay β here are smaller than the values obtained from electron transport measurements.[7] The discrepancy arises from the presence of high conductance percolation pathways in the AuNPs stripes and different inter-grain coupling strengths as well as the disordered arrangement in the AuNPs stripes.[8]

12. Signal to noise ratio determination

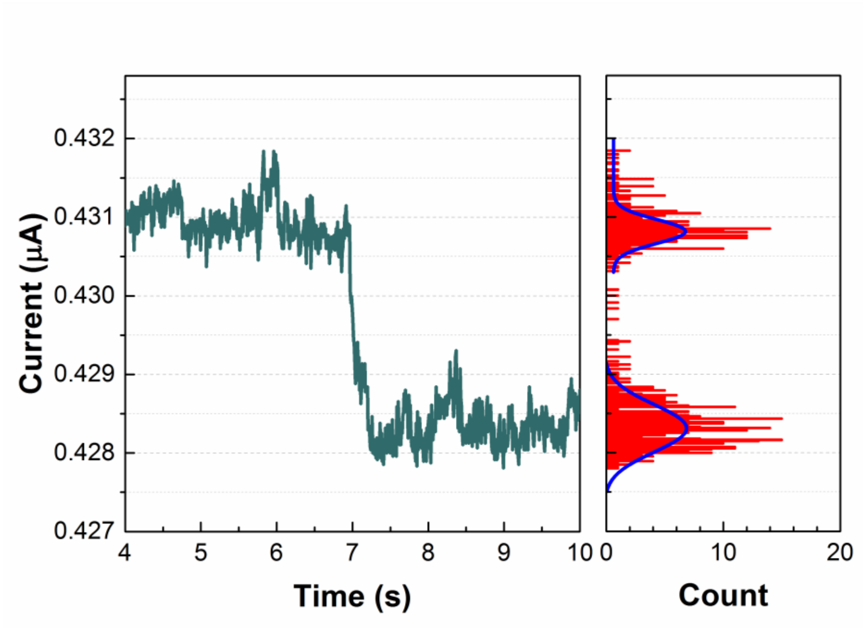

Figure S11. The step-like current signal (green curve) and the correspondingly histograms (red histogram). The blue curves on the right show the normal distribution fitting of the histograms.

The signal to noise ratio (SNR) was determined by the calculating the expectation value (μ) and the standard deviation (σ) of the normal distribution of this step-like signal. The current values before applying the strain and after applying the strain were plotted on a histogram and then were fitted by normal distribution. Expectation values (μ_1 and μ_2) and standard deviations (σ_1 and σ_2) can be extracted from the fitting curve. The signal value was defined as $S= |\mu_1- \mu_2|$. The noise value was defined by $N=\sqrt{(3\sigma_1)^2+ (3\sigma_2)^2}$. Finally SNR value is given by SNR=S/N.

Reference

[1] A. Sur, J. L. Lebowitz, J. Marro, M. H. Kalos, S. Kirkpatrick, J Stat Phys 1976, 15, 345.

[2] D. He, N. N. Ekere, Journal of Physics D: Applied Physics 2004, 37, 1848.

[3] C. K. Wu, K. L. Hultman, S. O'Brien, J. T. Koberstein, J Am Chem Soc 2008, 130, 3516.

[4] M. Pauly, B. P. Pichon, P.-A. Albouy, S. Fleutot, C. Leuvrey, M. Trassin, J.-L. Gallani, S. Begin-Colin, Journal of Materials Chemistry 2011, 21, 16018.
[5] D. Bruggeman, Annalen Der Physik 1936, 25, 645.
[6] G. Schmid, U. Simon, Chemical communications 2005, 697; M. Biancardo, A. J. Quinn, L. Floyd, P. M. Mendes, S. S. Briggs, J. A. Preece, C. A. Bignozzi, G. Redmond, J Phys Chem B 2005, 109, 8718.
[7] D. J. Wold, R. Haag, M. A. Rampi, C. D. Frisbie, J Phys Chem B 2002, 106, 2813; B. Xu, N. J. Tao, Science 2003, 301, 1221.
[8] K. H. Müller, G. Wei, B. Raguse, J. Myers, Physical Review B 2003, 68; H. Moreira, J. Grisolia, N. M. Sangeetha, N. Decorde, C. Farcau, B. Viallet, K. Chen, G. Viau, L. Ressier, Nanotechnology 2013, 24, 095701.